

Heterogeneous Catalyzed Reaction
Methanation of CO₂ Over a Ru/Al₂O₃ Catalyst
TKP4110

Group B4: Eva Aunet and Anine Bodsberg

Supervisor: Ask Lysne

July 28, 2022

1 Introduction

In this experiment, the CO_2 methanation reaction was investigated at various reaction conditions over a Ru-based catalyst. The methanation of CO_2 using green H_2 is of great interest, since it can reduce carbon emissions while producing methane that can be stored long-term or used as fuel.^[1] The experiment was conducted in a fixed bed quartz reactor in H_2 -rich surroundings at atmospheric pressure and temperatures of 350-370 °C. Micro gas chromatography (micro-GC) was used to analyze the effluent gas. The reaction order for CO_2 was determined by varying the partial pressure of CO_2 and assuming a power-law rate model, and the activation energy was determined by altering the reactor temperature and using Arrhenius' equation.

2 Experimental

The experimental setup consisted of four gas inlets, each connected to a mass-flow controller, and three-way valves at two different points, which directed the gas flow to go through either the reactor or the reactor bypass. After this, the gas flow was sent through a micro gas chromatograph for composition analysis, before being directed to a vent. A simplified flow sheet of the experimental setup is shown in figure 2.1.

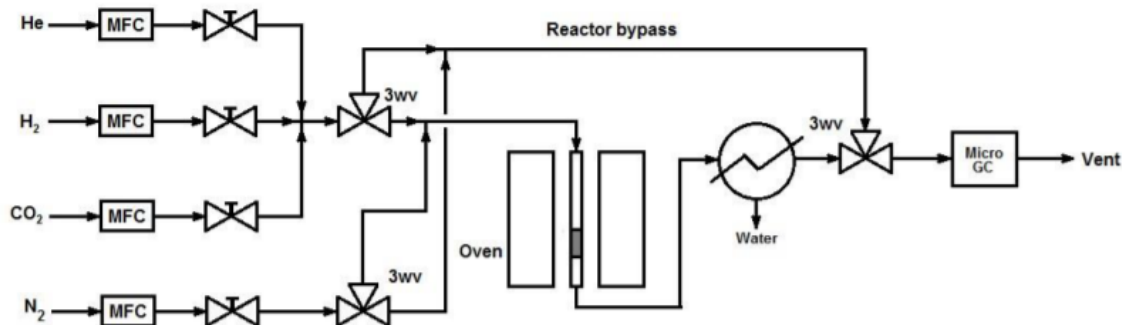


Figure 2.1: Simplified flow sheet of the catalyst testing apparatus with mass-flow controllers (MFC), three-way valves (3wv) and gas chromatograph (GC).

2.1 Preparation of the Reactor

The reactor was loaded with the $\text{Ru}/\text{Al}_2\text{O}_3$ catalyst (200 mg) containing 2 wt% Ru on a $\gamma\text{-Al}_2\text{O}_3$ support. To ensure isothermal conditions, the catalyst bed was diluted with inert SiC (800 mg). A plug of quartz wool was placed above and below the catalyst bed before the reactor was closed and placed inside the oven. The gas feed and outlet lines were then connected. To ensure proper monitoring of the reaction temperature, the thermocouple was placed inside the thermocouple holder in the reactor center. A leak test was performed by first running N_2 through the system and using a leak detection spray, and then running H_2 through the system and using a flammable gas detector. Finally, the reactor and reactor bypass was purged with N_2 to remove air from the system, before the oven was isolated and the condenser cooling water switched on.

2.2 Calibration of the Micro-GC

The three-way valves were set to direct the gas flow through the reactor bypass. The four gases were then introduced one by one to the system while continuously analyzing the flow with the micro-GC,

and the retention time of each component was determined.

2.3 Catalyst Pretreatment

To reduce Ru, a gas flow of 50 vol% H₂ in N₂ was sent over the catalyst bed while heating it from room temperature to 350 °C at a rate of 10 °C per minute.

2.4 Kinetic Experiment

The reactor temperature was kept constant at 350 °C while the gas composition was varied every 45 minutes for a total of three different gas compositions. This was done to determine the CO₂ reaction order. The gas composition was then kept constant, while the reactor temperature increased twice by 10 °C and was kept constant at each temperature for 45 minutes. This was done to determine the activation energy of the reaction. The kinetic experiment was performed under continuous micro-GC analysis of the gas flow.

2.5 System Shutdown

The system was purged with N₂ while cooling down to room temperature. Finally, the cooling water was switched off when the system reached room temperature.

3 Results and Discussion

The retention time for the different gas components measured with the micro gas chromatograph is presented in table 3.1.

Table 3.1: Retention time for different components measured with micro gas chromatography.

Component	Time [s]
He	30.9
H ₂	34.8
N ₂	65.8
CO ₂	310.0

The relative response factor, RRF_i , for CO₂ was determined by plotting the different molar flows of CO₂ during the micro-GC calibration against $\frac{A_{CO_2} \cdot F_{N_2}}{A_{N_2}}$, where A_{CO_2} is the peak area of CO₂, A_{N_2} is the peak area of N₂ and F_{N_2} is the constant molar flow rate of N₂. From linear regression analysis of the scatter plot, the relative response factor for CO₂ was found to be $RRF_{CO_2} = 0.68$. The plot is shown in figure B.1. The R^2 -value for this regression analysis was found to be 0.9964, which is very close to 1, and therefore suggests that the linear regression was a good fit for this scatter plot.

Figure 3.1 shows the CO₂ conversion plotted against the different partial pressures of CO₂ for the first three steps of the experiment. Each data point shows the average CO₂ conversion calculated from three measurements done for the same partial pressure, and the error bars shows the standard deviation for these measurements. The first data point shows a significantly larger deviation from the mean value than for the other two. This could mean that the system had not yet reached steady state in the first step of the experiment. The figure shows increasing levels of CO₂ conversion with the increase of CO₂ partial pressure. When looking at gaseous reactants, an increase in pressure means a higher frequency of molecular collisions, and thereby a higher reaction rate. This explains why the results shows a higher conversion of CO₂ when the partial pressure is increased.

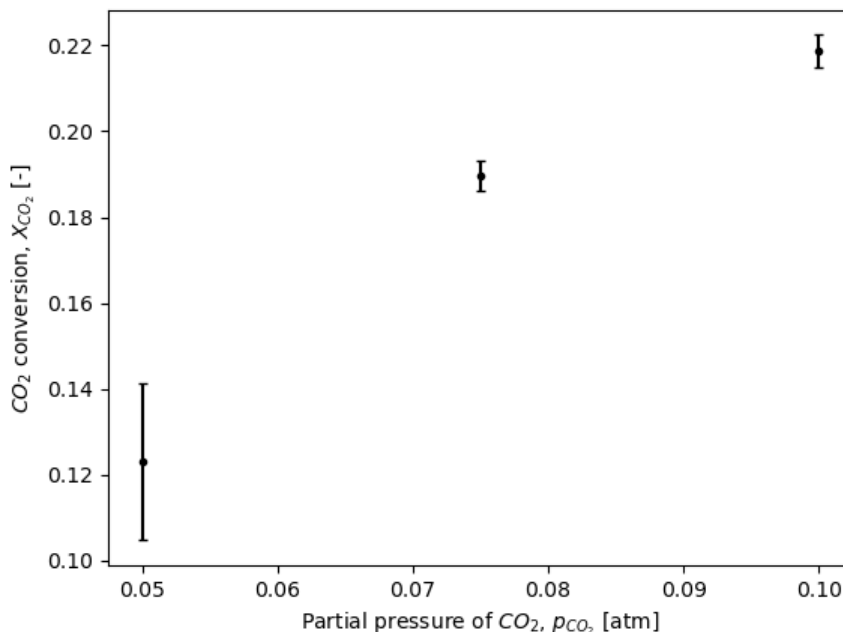


Figure 3.1: Conversion of CO₂ plotted against the CO₂ partial pressure in experimental steps 1-3.

Figure 3.2 shows the CO₂ conversion plotted against the different temperature levels for the last three steps of the experiment. Each data point shows the average CO₂ conversion levels calculated from three measurements done for the same temperature level, and the error bars shows the standard deviation for these measurements. In this figure, the deviation from the mean value is observed to increase with time and temperature, and it is possible that the system no longer operated at steady state conditions. The figure shows an increase in CO₂ conversion with temperature. Arrhenius' equation shows that an increase in temperature gives an increased rate constant. This means that more CO₂ will be converted with an increased temperature, which supports the results.

Figure 3.3 shows $\ln(-r_{\text{CO}_2})$ plotted against $\ln(p_{\text{CO}_2})$. From the slope of the linear regression line, the reaction order was found to be 1.87. The R^2 -value for this regression analysis was found to be 0.9634, and suggests that a linear regression model was a good fit.

Figure 3.4 shows $\ln(k)$ plotted as a function of $\frac{1}{T}$. By using the relation between k and T , described in equation A.5.2, and the linear regression line, the activation energy was found to be $E_a = 137.0 \text{ kJ mol}^{-1}$. Since the use of a catalyst lowers the activation energy, it is reasonable to assume that this experimental activation energy is lower than it would have been without the use of a catalyst. The R^2 -value for this regression analysis was found to be 0.9681, which points towards high quality of the regression analysis. The experimental value for the activation energy is similar to other values found in existing literature on CO₂ methanation over a Ru-based catalyst. Kuśmierz reports activation energies in the range from 82.6 ± 1.1 to $105.2 \pm 3.1 \text{ kJ mol}^{-1}$.^[2] These values are somewhat lower than the activation energy found in this experiment, which may be due to dissimilar experiment conditions. However, Kuśmierz' values are similar enough to conclude that the activation energy found in this experiment is reasonable.

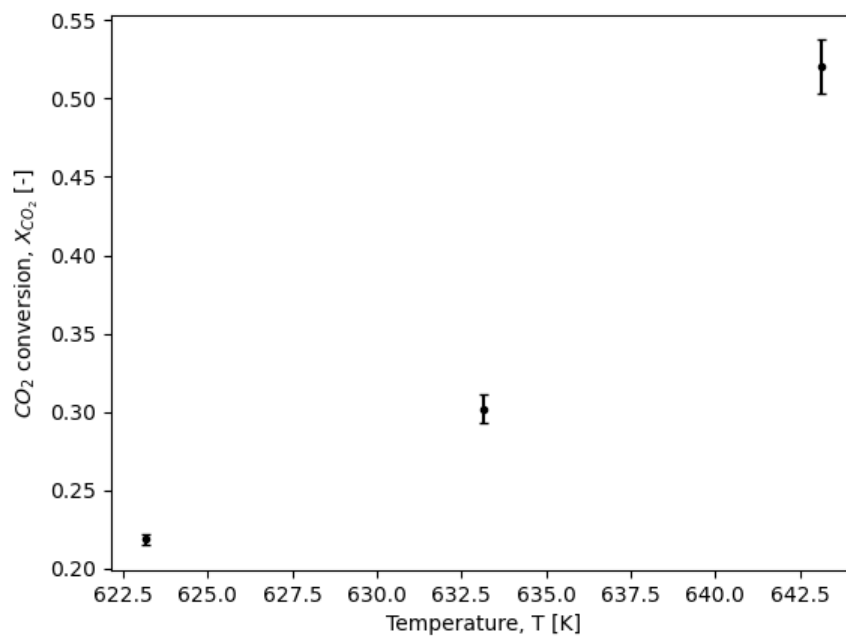


Figure 3.2: Conversion of CO₂ plotted against the temperature in experimental steps 3-5.

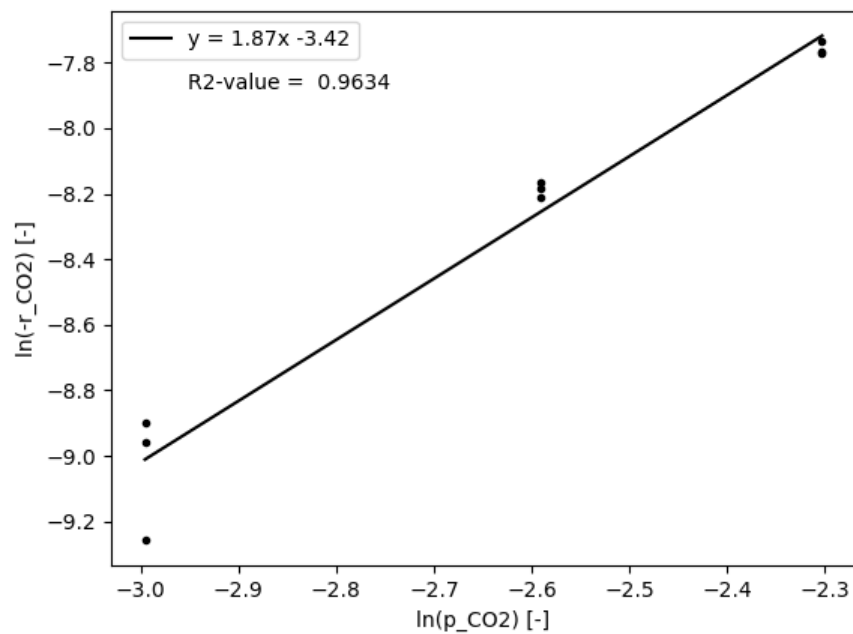


Figure 3.3: $\ln(-r_{\text{CO}_2})$ as a function of $\ln(p_{\text{CO}_2})$ for steps 1-3.

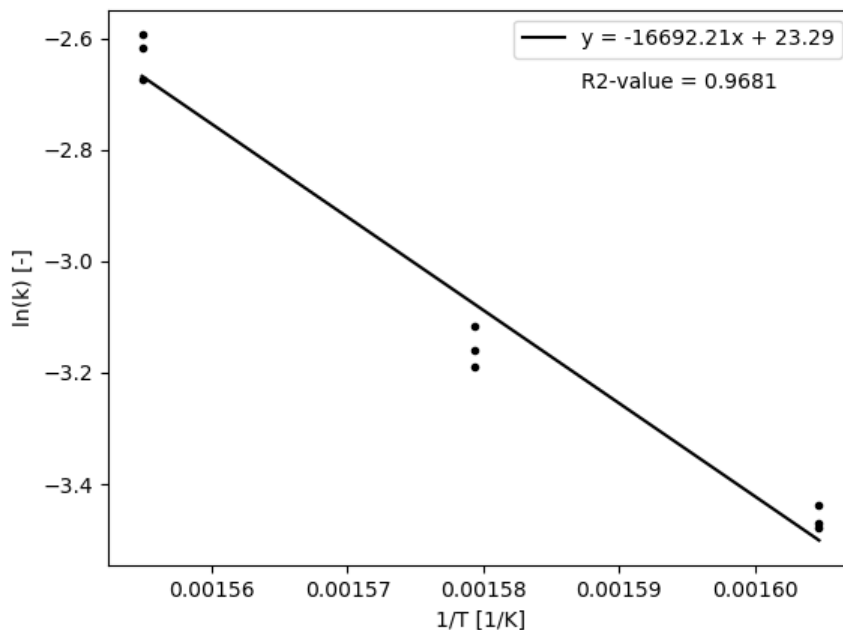


Figure 3.4: $\ln(k)$ as a function of $\frac{1}{T}$ for steps 3-5.

Several assumptions were made throughout the experiment. In order to calculate the molar flows from volume flows, ideal gas law was used. Real gases behave as ideal gases at high temperatures and low pressures, and because the experiment was conducted at high temperatures (350-370 °C) and the pressure was no more than 1 atm, this assumption is reasonable. Low conversion levels were also assumed, so that the kinetics of the methanation reaction could be described using a power-law rate model. However, the conversion level was calculated to be as high as 52 % at most, so this assumption does not hold up. Ideally, an integral reactor model should have been used when calculating $-r_{\text{CO}_2}$ to account for the changing CO_2 partial pressure through the reactor.

A possible source of error in this experiment is that the dwell time may have been too short for the reaction to reach steady state. The deviations in measured results shown particularly in the first data point of figure 3.1 and the last data point of figure 3.2 shows that the reaction probably did not operate at steady state throughout the entire experiment. Another source of error is leftover gas in the system from previous steps. This was taken into account by using the last and most stable measurements from the GC for each step. Lastly, the reactor temperature varied slightly and was often observed to be a few degrees higher than the programmed temperature levels. A higher temperature in the last two steps of the experiment would yield a lower value for $\frac{1}{T}$, which would give a steeper linear function in figure 3.4 and thus a higher value for the activation energy. This might explain why the activation energy found in this experiment is higher than those listed in Kuśmierz' article on hydrogenation of carbon dioxide over $\text{Ru}/\text{Al}_2\text{O}_3$ catalysts.

4 Conclusion

In this experiment, a CO₂ methanation reaction was performed with the use of a Ru-based catalyst. The temperature and CO₂ partial pressure was adjusted to determine the correlation between CO₂ conversion and the aforementioned variables, as well as the reaction order and activation energy. The experimental data, shown in figures 3.1 and 3.2, concluded that the CO₂ conversion increased with an increase of both temperature and CO₂ partial pressure. The reaction order was found to be 1.87. The activation energy was determined to be 137.0 kJ mol⁻¹, which is slightly higher than values found in existing literature on this particular experiment. An elevated value for the activation energy may be due to temperature fluctuations in the reactor. Other sources of error include leftover gas in the system from previous steps of the experiment, and that the system did not have enough time for the reaction to reach steady state before measurements were taken. In addition, the assumptions associated with the calculations of this experiment were of varying degree of accuracy.

References

- [1] Michael Specht, Jochen Brellocks, Volkmar Frick, Bernd Stuermer, Ulrich Zuberbuehler, Michael Sterner, and Gregor Waldstein. Storage of renewable energy in the natural gas grid. *Erdöl Erdgas Kohle*, 126, 2010.
- [2] Marcin Kuśmierz. Kinetic study on carbon dioxide hydrogenation over Ru/Al₂O₃ catalysts. URL <https://www.sciencedirect.com/science/article/pii/S0920586108001090>.
- [3] Ask Lysne. Methanation of CO₂ over a Ru/Al₂O₃ catalyst. URL https://folk.ntnu.no/preisig/HAP-Specials/Felles_lab/Experiments/RE6_heterogeneous_catalysed_reaction.pdf.

A Calculations

A.1 Molar Flow Rates

Table A.1.1 shows the MFC setpoints that were used in order to get the desired volume flows, along with volume fractions, total flows, temperatures, dwell time and reactor bypass.

Table A.1.1: Overview of the applied calibration and experimental conditions.^[3]

		MFC Setpoint [%] (a)				Volume Flow [mL/min] (b)				Volume Fraction [vol%] (b)				Total Flow [mL/min] (b)	Temperature			Dwell Time [min] (c)	Reactor Bypass
		CO ₂	H ₂	N ₂	He	CO ₂	H ₂	N ₂	He	CO ₂	H ₂	N ₂	He		Start [°C]	End [°C]	Ramp [°C/min]		
GC Calibration	Level 1	50.1	46.4	13.0	18.7	10	120	30	40	5	60	15	20	200	RT	RT	0	NA	Yes
	Level 2	71.5	46.4	13.0	16.3	15	120	30	35	7.5	60	15	17.5	200	RT	RT	0	NA	Yes
	Level 3	92.9	46.4	13.0	14.0	20	120	30	30	10	60	15	15	200	RT	RT	0	NA	Yes
Temperature Programmed Experiment	Reduction	0	39.1	45.0	0	0	100	100	0	0	50	50	0	200	RT	350	10	0	No
	Step 1	50.1	46.4	13.0	18.7	10	120	30	40	5	60	15	20	200	350	350	0	45	No
	Step 2	71.5	46.4	13.0	16.3	15	120	30	35	7.5	60	15	17.5	200	350	350	0	45	No
	Step 3	92.9	46.4	13.0	14.0	20	120	30	30	10	60	15	15	200	350	350	0	45	No
	Step 4	92.9	46.4	13.0	14.0	20	120	30	30	10	60	15	15	200	350	360	10	45	No
	Step 5	92.9	46.4	13.0	14.0	20	120	30	30	10	60	15	15	200	360	370	10	45	No
	Cool-down	0	0	45.0	0	0	0	100	0	0	0	100	0	100	370	RT	10	NA	No

(a) Determined from MFC calibration curves based on the provided calibration data.
 (b) At standard conditions (1 atm and 0 °C).
 (c) Dwell time at temperature program step end temperature.

RT = Room temperature
 NA = Not applicable

The MFC input signals in table A.1.1 were found using the following equations:

$$\begin{aligned}
 S_{\text{CO}_2} &= 4.28 \cdot F_{\text{CO}_2} + 7.34 \\
 S_{\text{H}_2} &= 0.366 \cdot F_{\text{H}_2} + 2.49 \\
 S_{\text{N}_2} &= 0.457 \cdot F_{\text{N}_2} - 0.709 \\
 S_{\text{He}} &= 0.474 \cdot F_{\text{He}} - 0.254
 \end{aligned}
 \tag{A.1.1}$$

Here, F is the flow rate and S is the MFC input signal. These equations were found from linear regression of the MFC input signals as functions of the flow rates, which were plotted using the given calibration data.^[3] The calibration curves are shown in figures A.1.1 - A.1.4.

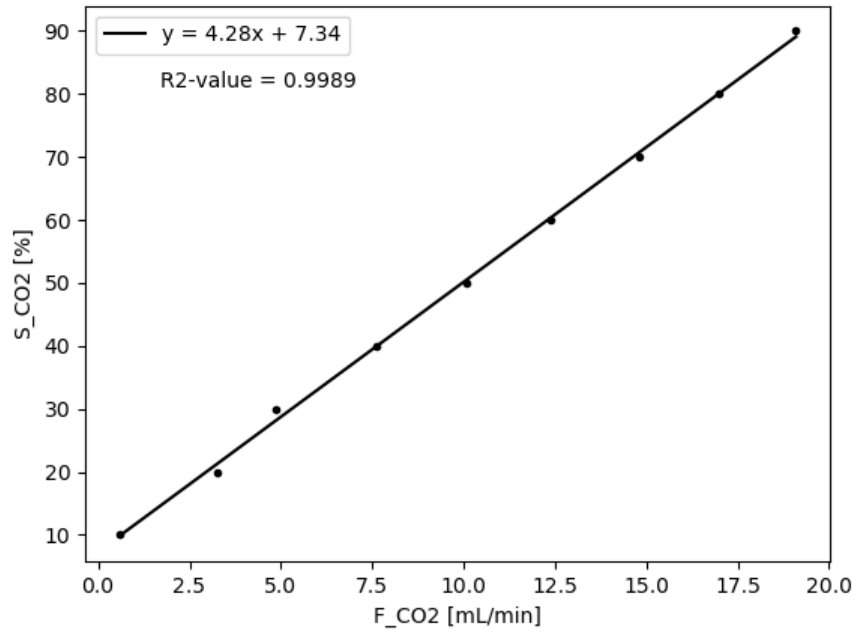


Figure A.1.1: s_{CO_2} as a function of F_{CO_2} .

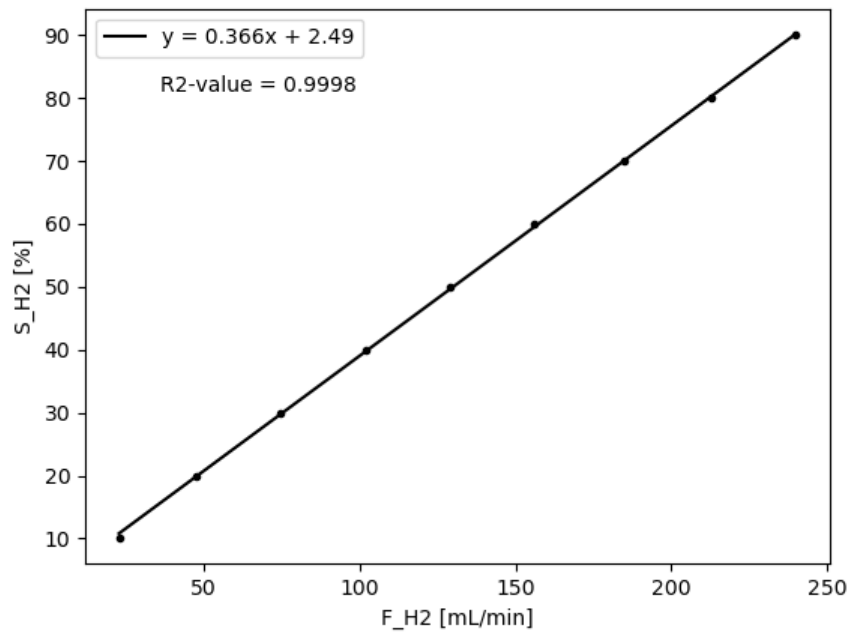


Figure A.1.2: s_{H_2} as a function of F_{H_2} .

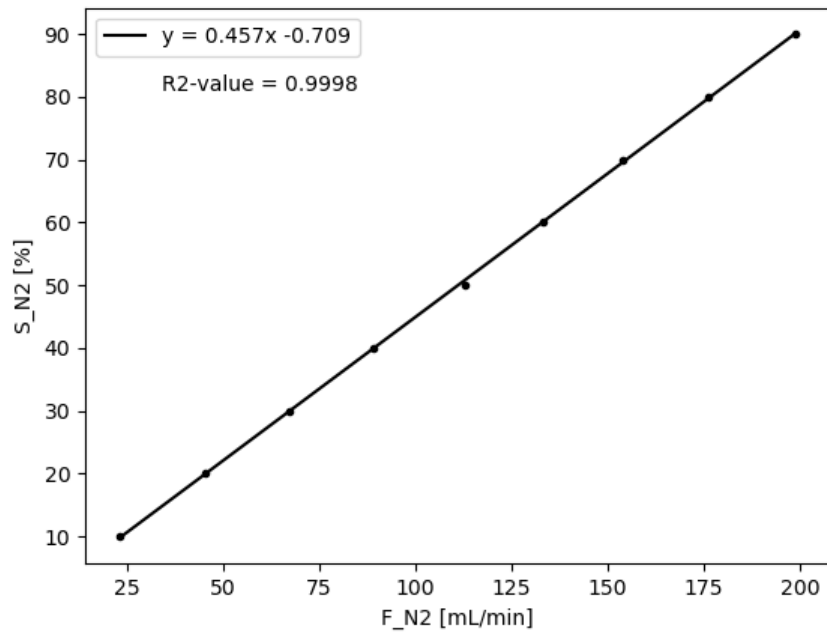


Figure A.1.3: S_{N_2} as a function of F_{N_2} .

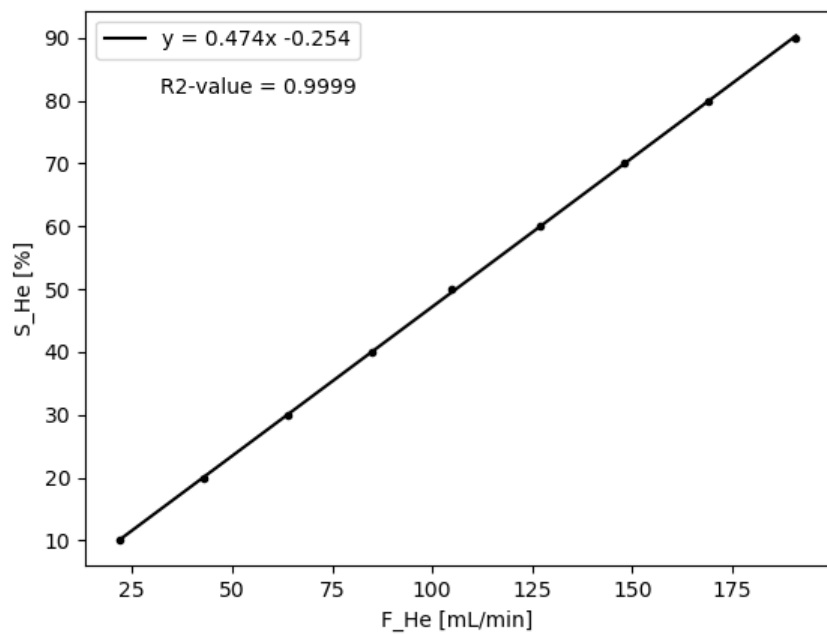


Figure A.1.4: S_{He} as a function of F_{He} .

A.2 Gas Chromatography

To find the CO₂ conversion, data from gas chromatography was used. But first, the GC apparatus was calibrated. This was done by analyzing gas mixtures with known compositions, and from this determining the response factor of a component along with its retention time. The response factor RF_i for a compound i can be expressed as

$$RF_i = \frac{A_i}{y_i}, \quad (\text{A.2.1})$$

where A_i is the peak integration area and y_i is the molar fraction. In this experiment, the internal standard method was used to calibrate the GC apparatus, with the inert gas N₂ functioning as the internal standard. The response factor for the internal standard RF_{IS} was then used to define a relative response factor RRF_i :

$$RRF_i = \frac{RF_i}{RF_{IS}}. \quad (\text{A.2.2})$$

Combining equation (A.2.1) and (A.2.2) and introducing molar flow F gives:

$$RRF_i = \frac{A_i y_{IS} F_{tot}}{y_i A_{IS} F_{tot}} = \frac{A_i F_{IS}}{A_{IS} F_i}. \quad (\text{A.2.3})$$

The molar flow rate F of component i is then found by solving for F_i :

$$F_i = \frac{A_i F_{IS}}{A_{IS} RRF_i}. \quad (\text{A.2.4})$$

The conversion of CO₂, X_{CO_2} , was calculated using equation (A.2.5):

$$X_{CO_2} = \frac{F_{CO_2}^0 - F_{CO_2}}{F_{CO_2}^0}. \quad (\text{A.2.5})$$

A.3 Reaction Rate

The rate of CO₂ consumption, $-r_{CO_2}$, is given by

$$-r_{CO_2} = kp_{CO_2}^a p_{H_2}^b, \quad (\text{A.3.1})$$

where k is the rate constant, p is the partial pressure of the reactants, and a and b are the reaction order for CO₂ and H₂ respectively. The reaction rate can be considered independent of the partial pressure of H₂ in a H₂-rich atmosphere ($b = 0$), and thus equation (A.3.1) becomes

$$-r_{CO_2} = kp_{CO_2}^a. \quad (\text{A.3.2})$$

The reaction rate is related to the conversion level by

$$-r_{CO_2} = \frac{F_{CO_2}^0 X_{CO_2}}{\Delta W}, \quad (\text{A.3.3})$$

where $F_{\text{CO}_2}^0$ is the molar flow rate of CO_2 at the reactor inlet, X_{CO_2} is the CO_2 conversion and ΔW is the mass of the applied catalyst.

A.4 Reaction Order

Linearization of equation (A.3.2) gives

$$\ln(-r_{\text{CO}_2}) = \ln(k) + a \cdot \ln(p_{\text{CO}_2}). \quad (\text{A.4.1})$$

Plotting $\ln(-r_{\text{CO}_2})$ as a function of $\ln(p_{\text{CO}_2})$, and performing linear regression analysis, gives the reaction order, a , as the slope of the straight line function, and the rate constant, k , as the intersection between the straight line and the y-axis.

A.5 Activation Energy

The activation energy E_A was found by measuring $-r_{\text{CO}_2}$ at different temperatures and determining the rate constant k from equation (A.3.2). Arrhenius' equation given in (A.5.1)

$$k = Ae^{\frac{-E_a}{RT}} \quad (\text{A.5.1})$$

was linearized to get equation A.5.2.

$$\ln k = \ln A - \frac{E_a}{R} \frac{1}{T}. \quad (\text{A.5.2})$$

When plotting $\ln k$ against $\frac{1}{T}$, $\frac{-E_a}{R}$ is the slope of the curve and $\ln A$ is the intercept value.

B GC Calibration

The gas chromatograph was calibrated for three different molar flow rates of CO_2 , which were plotted against $\frac{A_{\text{CO}_2} \cdot F_{\text{N}_2}}{A_{\text{N}_2}}$. The result is shown in figure B.1. The relative response factor for CO_2 , RRF_{CO_2} , is given by the slope of the linear regression function, and found to be 0.68.

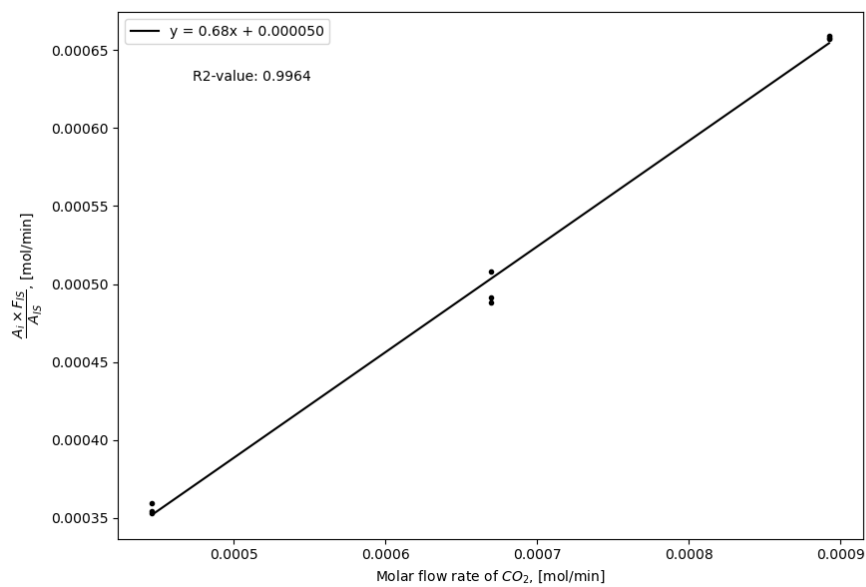


Figure B.1: Linear regression plot of the micro gas chromatography calibration. The slope of the function was found to be 0.68.